JOURNAL OF VIROLOGY, Dec. 1998, p. 9806–9817 Vol. 72, No. 12
0022-538X/98/$04.00+0
Copyright © 1998, American Society for Microbiology. All Rights Reserved.

The Equine Herpesvirus 1 IR6 Protein That Colocalizes with Nuclear Lamins Is Involved in Nucleocapsid Egress and Migrates from Cell to Cell Independently of Virus Infection

NIKOLAUS OSTERRIEDER,[1,2]* ANTONIE NEUBAUER,[1,3] CHRISTINE BRANDMÜLLER,[1] OSKAR-RÜGER KAADEN,[1] AND DENNIS J. O'CALLAGHAN[3]

Institute for Medical Microbiology, Infectious and Epidemic Diseases, Ludwig-Maximilians-Universität München, D-80539 Munich,[1] and Institute of Molecular and Cellular Virology, Friedrich-Loeffler-Institutes, Federal Research Centre for Virus Diseases of Animals, D-17498 Insel Riems,[2] Germany, and Department of Microbiology and Immunology, Louisiana State University Medical Center, Shreveport, Louisiana 71130[3]

Received 15 June 1998/Accepted 10 September 1998

The equine herpesvirus 1 (EHV-1) IR6 protein forms typical rod-like structures in infected cells, influences virus growth at elevated temperatures, and determines the virulence of EHV-1 Rac strains (Osterrieder et al., Virology 226:243–251, 1996). Experiments to further elucidate the functions and properties of the IR6 protein were conducted. It was shown that the IR6 protein of wild-type RacL11 virus colocalizes with nuclear lamins very late in infection as demonstrated by confocal laser scan microscopy and coimmunoprecipitation experiments. In contrast, the mutated IR6 protein encoded by the RacM24 strain did not colocalize with the lamin proteins at any time postinfection (p.i.). Electron microscopical examinations of ultrathin sections were performed on cells infected at 37 and 40°C, the latter being a temperature at which the IR6-negative RacH virus and the RacM24 virus are greatly impaired in virus replication. These analyses revealed that nucleocapsid formation is efficient at 40°C irrespective of the virus strain. However, whereas cytoplasmic virus particles were readily observed at 16 h p.i. in cells infected with the wild-type EHV-1 RacL11 or an IR6-recombinant RacH virus (HIR6-1) at 40°C, virtually no capsid translocation to the cytoplasm was obvious in RacH- or RacM24-infected cells at the elevated temperature, demonstrating that the IR6 protein is involved in nucleocapsid egress. Transient transfection assays using RacL11 or RacM24 IR6 plasmid DNA and COS7 or Rk_{13} cells, infection studies using a gB-negative RacL11 mutant (L11ΔgB) which is deficient in direct cell-to-cell spread, and studies using lysates of IR6-transfected cells demonstrated that the wild-type IR6 protein is transported from cell to cell in the absence of virus infection and can enter cells by a yet unknown mechanism.

The alphaherpesvirus equine herpesvirus 1 (EHV-1) is the major cause of virus-induced abortion in horses. Additionally, the agent causes respiratory and neurological symptoms (1, 13, 18). Of the more than 76 proteins encoded by EHV-1, most share extensive homology with the prototype member of the virus subfamily, herpes simplex virus type 1 (HSV-1) (30). Among the open reading frames (ORFs) that are not present in HSV-1, the IR6 gene (gene 67) and gene product have been identified (2, 17, 29). Structural homologs of the EHV-1 IR6 protein have been described on the basis of nucleotide sequence analyses in equine herpesvirus 4 (EHV-4), bovine herpesvirus 1 (BHV-1), and canine herpesvirus (CHV) (11, 14, 26, 31). The EHV-1 IR6 gene is present as a diploid gene in both inverted repeat regions in wild-type EHV-1 strains, and its protein product has been shown to form filamentous rod-like structures that localize primarily to the soluble fraction of the cytoplasm in infected cells. In addition, the IR6 protein forms a meshwork surrounding the nuclei of infected cells starting at 6 h postinfection (p.i.), is found in the nuclei of infected cells, and is incorporated into viral nucleocapsids (3, 17, 19). Analysis of EHV-1 viruses that express a mutated IR6 protein has demonstrated that the structure of the IR6 protein is important for its function (19, 20). A viral mutant that is devoid of both copies of the IR6 gene, EHV-1 strain RacH, is apathogenic for the natural host and for laboratory animals. Upon insertion of the IR6 gene, however, the generated IR6 recombinant RacH virus (HIR6-1) was as virulent as the wild-type RacL11 virus (8, 12, 20). Moreover, the temperature-sensitive phenotype of the IR6-negative RacH and the Rac plaque isolates expressing a mutated IR6 protein (RacM24 and RacM36) was restored by the insertion of one copy of the wild-type IR6 gene into the RacH virus (20).

Despite the intensive phenotypical characterization of individual strains expressing various forms of the IR6 protein, the function of the protein remained enigmatic. The observed aggregation of the IR6 protein to the rod-like structures led to the hypothesis that it could interact with cellular proteins that form the cytoskeleton (17). However, no association of the IR6 protein with the investigated proteins actin, tubulin, vimentin, dynein, kinesin, and desmin could be shown (17, 19, 29). To date, the nuclear lamins which represent members of the intermediate filament family have not been analyzed for a putative aggregation with the IR6 protein, although they are expressed in all eukaryotic cells. In vertebrate somatic cells, two major types of nuclear lamins (type B1-B2 and type A/C) can be distinguished, although they are structurally and functionally homologous and may have arisen from the same ancestral gene (reviewed in reference 6). The lamins are located on the nucleoplasmic side of the inner nuclear membrane, are associated with chromatin, and form a meshwork which determines the nuclear architecture. In addition, nuclear lamins play an important role during mitosis and are phosphorylated in the M

* Corresponding author. Mailing address: Institute of Molecular and Cellular Virology, Friedrich-Loeffler-Institutes, Federal Research Centre for Virus Diseases of Animals, D-17498 Insel Riems, Germany. Phone: 49-38351-7266. Fax: 49-38351-7151. E-mail: klaus.osterrieder@rie.bfav.de.

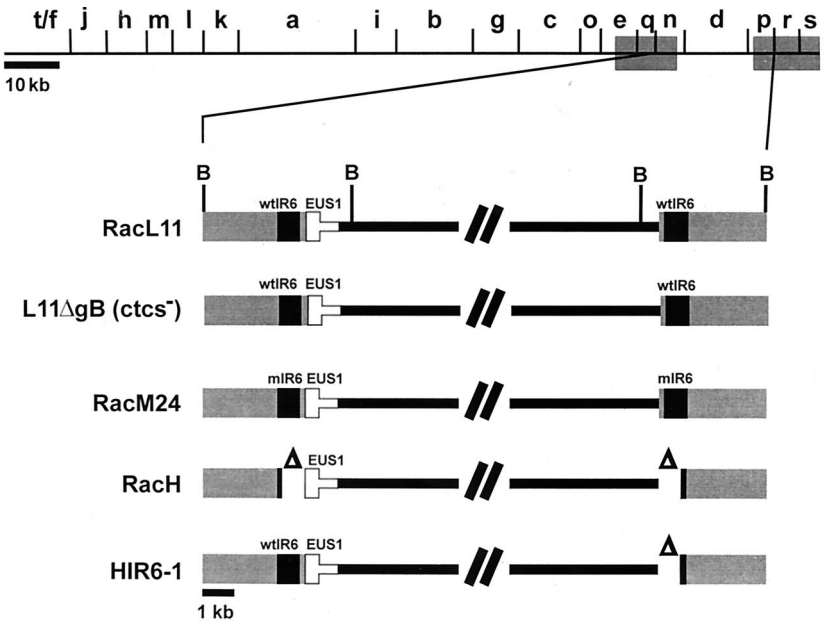

FIG. 1. Schematic diagram of the genotypes of the viruses used in this study (15, 19, 20). Shown are the *Bam*HI map of EHV-1 strain RacL11 and the magnifications of the U_S and inverted repeat regions of strains RacL11, RacM24, RacH, and the HIR6-1 virus. The HIR6 virus is a recombinant RacH virus into which one copy of the wild-type IR6 virus was inserted (20). Also shown is the organization of the gB-negative EHV-1 mutant L11ΔgB (15), which is deficient in direct cell-to-cell-spread (ctcs$^-$) but expresses the wild-type IR6 protein. *Bam*HI restriction fragment designations are given, and wild-type (wt) as well as mutated (m) IR6 genes (amino acid 134: Leu→Pro) are indicated. Also shown is the location of the EUS1 gene (gene 68), the EHV-1 U_S2 homolog (30). The deletion of both copies of the IR6 gene in strain RacH is marked (Δ). The scale is given in kilobase pairs (kb). The U_S region in the magnification is not drawn to scale.

phase of the cell cycle by the cdc2 protein kinase (25). During mitosis, B-type lamins remain associated with the nuclear membrane, whereas A-type lamins disintegrate and are present as soluble oligomers (16).

This study addresses the functional characterization of the EHV-1 IR6 gene product and its colocalization with members of the intermediate filament family, the nuclear lamins. To this end, transient transfection assays of IR6 genes, confocal laser scanning microscopy, coimmunoprecipitation analyses, and electron microscopy were performed using different EHV-1 strains which express wild-type or mutated forms of the IR6 protein. It is shown that the wild-type IR6 protein is transported from cell to cell independently of viral infection, colocalizes with nuclear lamins late in infection, and encodes a function that facilitates the egress of viral nucleocapsids.

MATERIALS AND METHODS

Cells and viruses. The equine dermal cell line Edmin337 (8) as well as Rk_{13} and EHV-1 gB-expressing TCgBf cells (15) were maintained in Dulbecco's minimal essential medium (DMEM) supplemented with 10% fetal calf serum (FCS). EHV-1 strains RacL11, RacM24, and RacH, as well as the IR6-recombinant RacH virus (HIR6-1), were grown and titrated as previously described (19, 20). The gB-negative RacL11 mutant (L11ΔgB) that expresses *Escherichia coli* β-galactosidase instead of the gB ORF and that is deficient in cell-to-cell spread of infectivity was propagated on complementing TCgBf cells (15) before infection of noncomplementing cells. For detection of β-galactosidase activity in L11ΔgB-infected cells, cells were fixed with acetone or methanol and stained with β-galactosidase staining solution [final concentrations: 300 μg of Bluo-Gal (Gibco-BRL)/ml, 5 mM $K_4Fe(CN)_6$, 5 mM $K_3Fe(CN)_6$, 2 mM $MgCl_2$, 0.1% Triton X-100 in phosphate-buffered saline (PBS)]. A diagram of the genotypes of the different EHV-1 used in this study is presented in Fig. 1.

Plasmids. The recombinant plasmids pDIR6L and pDIR6M24, which contain the RacL11 or the RacM24 IR6 ORF, respectively, under the control of the cytomegalovirus immediate-early promoter, have been described previously (19). The plasmid pCβ$^+$ was constructed by inserting the *E. coli lacZ* gene released from vector pSV-β-Galactosidase (Gibco-BRL) into the vector pcDNAI/Amp (Invitrogen) and was used as the reporter plasmid in transient transfection experiments.

Electron microscopy. Rk_{13} or Edmin337 cells were seeded in 75-cm^2 cell culture flasks and infected with the indicated viruses at a multiplicity of infection (MOI) of 5. At 4 or 16 h after infection, cells were fixed with 2% glutaraldehyde in PBS for 2 h and washed in PBS. Cells were postfixed with 2% OsO_4 in PBS, washed thoroughly with PBS, and embedded in 1% agarose. Cells were dehydrated stepwise in solutions containing 50 to 100% ethanol. After equilibration in propylene oxide, cells were embedded in Epon (Fluka) and polymerized for 2 to 4 days at 45 to 60°C. Sections of 50 to 80 nm were cut with a microtome, and the sections were counterstained with 2% phosphotungstic acid in PBS and analyzed with a Zeiss EM 10C/CR electron microscope (21).

Transient transfection assays. Transfections of Rk_{13} cells were done by lipotransfection or calcium phosphate precipitation exactly as previously described (15), and 1 μg of the respective plasmids was transfected into 5×10^5 cells seeded on coverslips. To prevent cell division in transiently transfected cells, cells were incubated after transfection in DMEM without addition of FCS. IR6 import assays were done exactly as described by Elliott and O'Hare in the case of HSV-1 VP22 by extraction with 0.4 M NaCl (4). Briefly, 1×10^6 Rk_{13} cells were transfected with 10 μg of pDIR6L or pDIR6M24, and cell-free lysates were prepared at 72 h after transfection and added to the medium of Rk_{13} cells that had been seeded 24 h before. The lysate of approximately 3×10^3 transfected cells was used to overlay 1×10^4 freshly seeded Rk_{13} cells. At different times after addition of the lysate, uptake of the IR6 protein into cells was determined by indirect immunofluorescence (IF) using the anti-IR6 antiserum (see below). Before inspection in a fluorescence microscope, nuclei were stained with propidium iodide (10^{-6} M in PBS).

Antibodies. The anti-IR6 antibody (17) was used at a 1:1,000 dilution. Anti-β-galactosidase monoclonal antibodies (MAbs) (Boehringer) were purchased and used according to the manufacturer's instructions. Anti-lamin MAbs were kindly provided by Georg Krohne, University of Würzburg, Germany. The antibodies X67, X167, and R27 react with different epitopes of type A lamins, whereas MAb X223 is specific for B-type lamins (7). Each of the lamin antibodies was used at a dilution of 1:200 in Western blot and immunofluorescence analyses. Anti-EHV-1 gB MAb 4B6 and anti-gD polyclonal rabbit antibodies have been previously described (5, 15).

Immunoprecipitation and Western blotting. Rk_{13} cells were infected at an MOI of 2 with RacL11, RacM24, RacH, or the IR6-recombinant virus HIR6-1. At 16 h after infection, cell lysates were prepared exactly as previously described (15). The cell lysates were adjusted to equal protein concentrations of 5 mg per ml as determined by the BCA kit (Pierce). A mixture of preimmune rabbit serum (10 μl) and the supernatant of an irrelevant hybridoma (500 μl) was added to 500 μl of cell lysate. The mixture was incubated for 1 h on ice, and 80 μl of a protein A-agarose slurry (Bio-Rad) was added for 1 h on ice. After centrifugation, the supernatant was diluted with NET buffer (20 mM Tris-Cl [pH 7.6]; 150 mM NaCl; 5 mM EDTA; 0.1% Nonidet P-40; 0.25% gelatin; 0.02% NaN_3) to 2.5 ml (27). Five hundred microliters of the suspension was mixed with 5 μl of the anti-IR6 antiserum or 5 μl of the anti-lamin A antibodies. The mixture was

incubated on ice for 1 h, and protein-antibody complexes were precipitated with protein A-agarose as described above. After four washing steps in NET buffer, beads were suspended in protein sample buffer (27), and the samples were heated to 56°C for 2 min. Protein samples were separated by sodium dodecyl sulfate-polyacrylamide gel electrophoresis (SDS-PAGE) (10). For Western blot analysis, proteins were transferred to nitrocellulose membranes (Biometra) by the semidry method (9). Free binding sites on the sheets were blocked by the addition of 10% nonfat dried milk in PBS containing 0.05% Tween (PBST) before the antibodies (suspended in PBST) were added. Bound antibodies were detected with anti-rabbit (or anti-mouse) immunoglobulin G (IgG) alkaline phosphatase conjugates (Sigma) and visualized with nitroblue tetrazolium and 5-bromo-4-chloro-3-indolyl phosphate (Sigma).

Immunofluorescence and confocal laser scanning microscopy. For indirect IF analyses, transfected or infected cells were fixed with ice-cold acetone or methanol for 5 min at different times after transfection or infection. The cells were rehydrated with PBS for 10 min and incubated with anti-IR6 monospecific rabbit antiserum (17) for 30 min after a 45-min blocking period using 10% FCS diluted in PBS. In some experiments, MAbs against β-galactosidase or EHV-1 gB were mixed with the anti-IR6 antibody. After thorough washing (twice for 10 min in PBS), an anti-rabbit IgG fluoroisothiocyanate (FITC) conjugate alone or together with an anti-mouse IgG TRITC conjugate (Sigma) was added for 30 min. For detection of nuclear lamins, coverslips were incubated with anti-IR6 and anti-lamin antibodies. After two washes, an anti-mouse IgG biotin conjugate or anti-mouse Cy3 conjugate (Jackson Laboratories) was added for 45 min. In the case of biotinylated antibodies, another two washes with PBS followed, and bound biotin was detected by streptavidin-phycoerythrin (Sigma). After two final washing steps, the samples were analyzed with a fluorescence microscopy (Zeiss Axiovert 25) or by confocal laser scanning microscopy (Zeiss LSM 510).

RESULTS

The EHV-1 IR6 protein colocalizes with nuclear lamins. The appearance of the EHV-1 IR6 protein-specific rod-like structures in infected cells suggested a colocalization with proteins that influence the cell's architecture (17, 19, 20, 29). To test the hypothesis that the IR6 protein colocalizes with lamin proteins which are associated with the inner nuclear membrane and are involved in cell division (6), two different approaches were taken.

First, cells infected with either RacL11 encoding the wild-type IR6 protein, with RacM24 encoding a mutated form of the IR6 protein (amino acid 134: Leu→Pro), or with the RacH virus which lacks the IR6 ORFs were labeled with both anti-IR6 and a mixture of anti-lamin A and B antibodies, and analyzed by laser confocal microscopy from 2 to 18 h p.i. The results of the indirect IF analyses demonstrated a colocalization of the IR6-specific fluorescence (FITC fluorescence: green) and the lamin-specific fluorescence (phycoerythrin fluorescence: red) in RacL11-infected cells at 12 h p.i. (Fig. 2A). Both fluorescences were associated with thread-like structures that are typical of those formed by the wild-type IR6 protein late in infection (17, 19, 20, 29). When the IR6-specific and lamin-specific fluorescences were superimposed, the staining patterns of both the RacL11 IR6 and the lamin proteins were identical as demonstrated by the yellow appearance of the structure (Fig. 2A). It must be noted, however, that the colocalization of the IR6 protein with nuclear lamins did not start before 8 to 10 h p.i. (Fig. 2B) but could be observed from that time until the end of the observation period of 18 h p.i. (data not shown). In contrast, a colocalization of nuclear lamins and the mutated IR6 protein expressed by RacM24 could not be observed even at very late time points p.i., and as reported previously the IR6 protein exhibited an even to granular appearance in infected cells (Fig. 3A). In RacH-infected cells, the nuclear lamins exhibited their normal staining pattern of a nuclear rim fluorescence (28), although the examined cells were infected, as visualized with an anti-gD polyclonal rabbit antiserum (Fig. 3B). These results indicated that the wild-type IR6 protein colocalizes with nuclear lamins late in infection, whereas the mutated IR6 protein expressed by RacM24 does not colocalize with nuclear lamins. In addition, intact lamin structures were

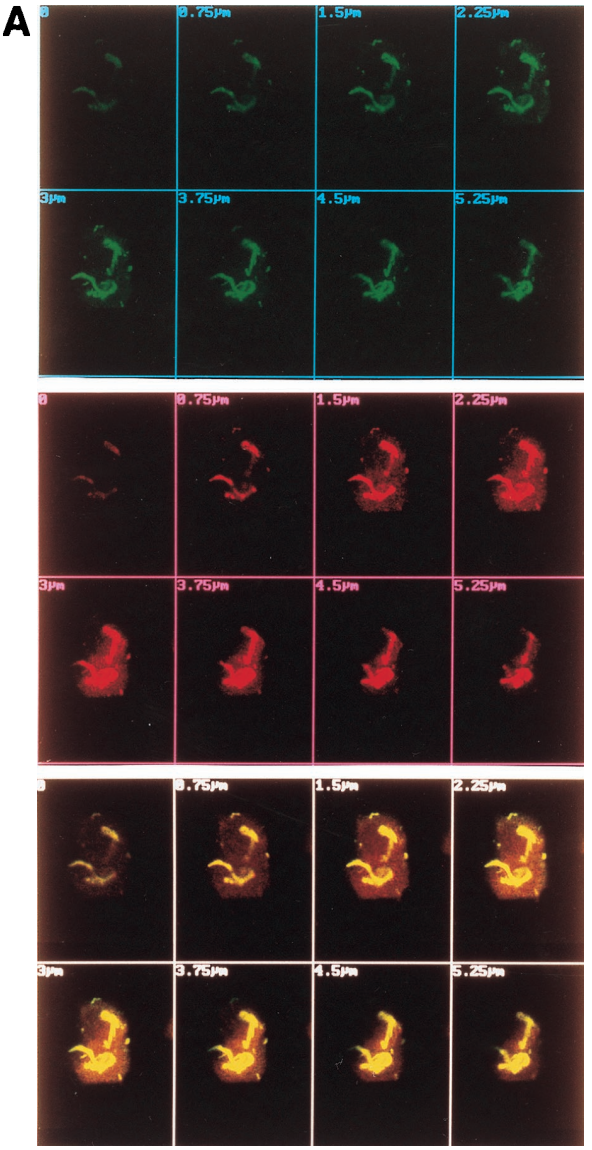

FIG. 2. Laser confocal scanning images of RacL11-infected Rk_{13} cells fixed at 12 h p.i. (A) or 2 to 10 h p.i. (B). Cells were fixed with acetone, and slides were probed with anti-IR6 antibodies and a mixture of anti-lamin antibodies as described in Materials and Methods. Green FITC fluorescence (IR6) and red phycoerythrin or Cy3 fluorescence signals (lamins) were recorded separately by using appropriate filters. Overlay of the IR6 and lamin fluorescent signals is shown in yellow. At the 12-h time point (A), serial 750-nm sections through an infected cell are shown.

observed in RacM24-infected cells even at 18 h p.i. (Fig. 3A) as was the case in RacH- (Fig. 3B) or mock-infected cells.

To confirm the immunofluorescence data and to identify more precisely which of the lamin proteins aggregates with the viral IR6 protein, infected cell lysates were subjected to immunoprecipitation followed by Western blotting. RacL11-, RacM24-, and RacH-infected cell lysates were prepared at 16 h p.i. and precipitated with either anti-IR6 antibodies or a mixture of MAbs specific for type A lamins (7). After separation of the immunoprecipitates by SDS–10% PAGE, proteins were transferred to nitrocellulose sheets which were probed with the anti-IR6 or anti-lamin A antibodies. When the immunoprecipitates obtained with the anti-IR6 antibody were probed with the anti-

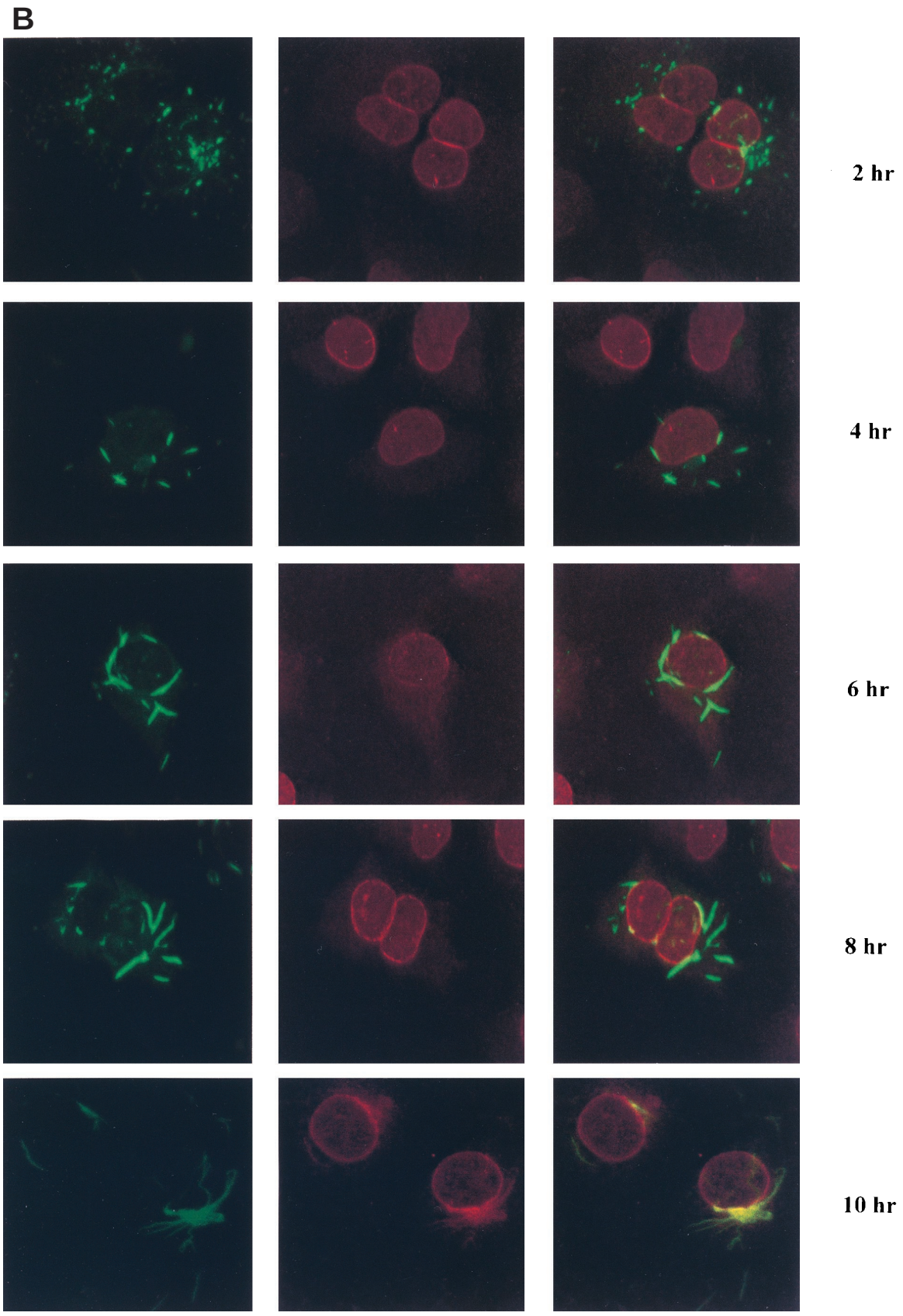

FIG. 2—*Continued.*

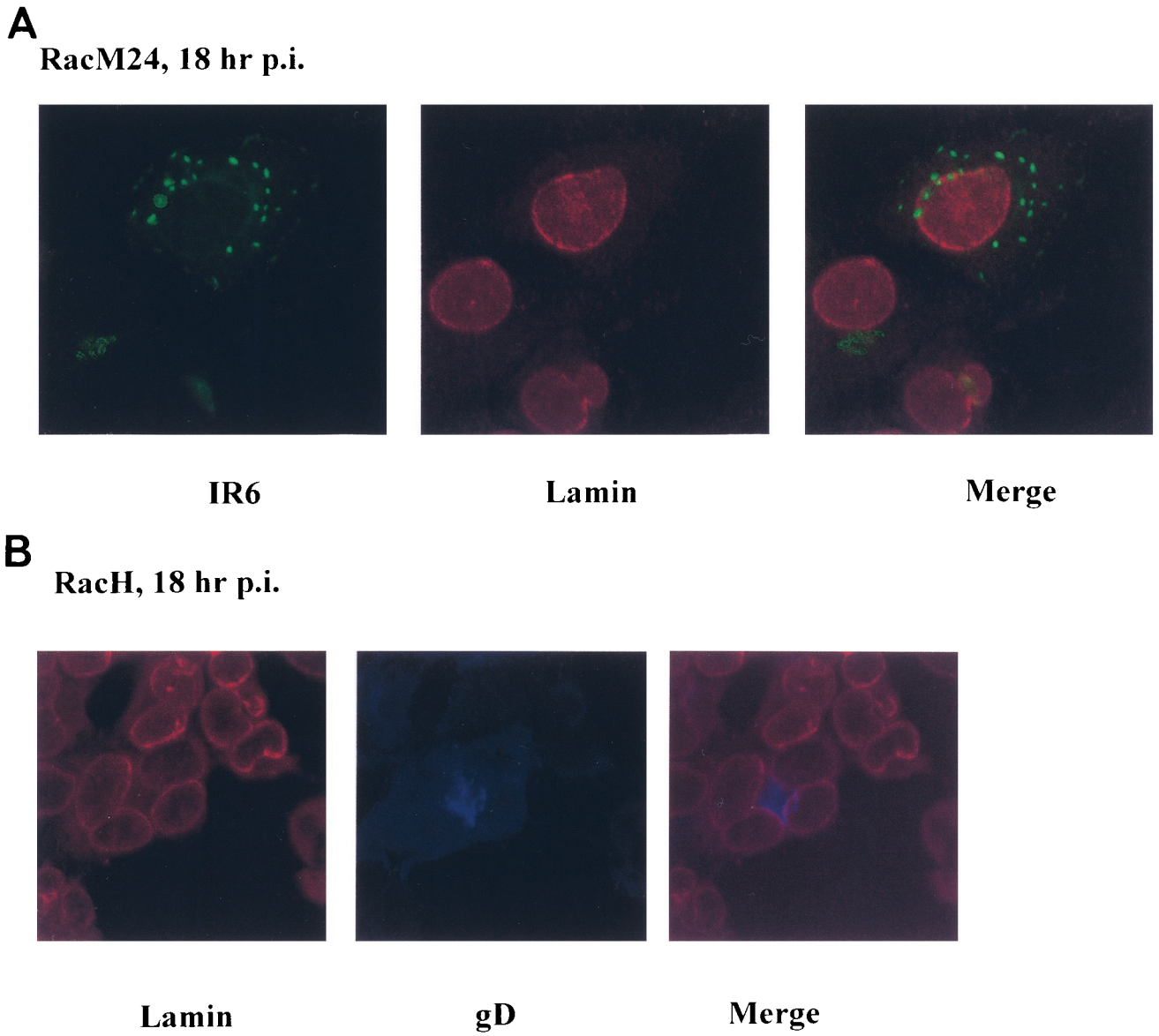

FIG. 3. Laser confocal scanning images of RacM24- (A) or RacH-infected cells (B) at 18 h p.i. Cells were reacted with anti-lamin antibodies which were detected with anti-mouse IgG Cy3 conjugate (red). In RacM24-infected cells, simultaneous staining with the anti-IR6 antibody detected with an anti-rabbit IgG FITC (green) was performed. In the case of the IR6-negative RacH virus, infection of cells was analyzed with anti-gD antibody detected with anti-rabbit IgG Cy5 (blue). No disintegration of nuclear lamins or their colocalization with RacM24 IR6 could be observed.

IR6 antibody in an immunoblot, bands of M_r 31,000 to 33,000 were readily detected in RacL11- and RacM24-infected cells, whereas the IR6-specific bands were absent in RacH-infected cells (Fig. 4A). Additionally, the IR6 protein was detected in RacL11-infected cell lysates that had been subjected to immunoprecipitation with the anti-lamin A antibodies (Fig. 4A). In contrast, the IR6 protein was not precipitated by the anti-lamin A antibodies in cells infected with RacM24 (expressing a mutated IR6 protein), with the IR6-negative RacH virus, or in cells that had been mock-infected (Fig. 4A). Western blot analysis of mock-infected Rk_{13} cell lysates using the anti-lamin A antibodies revealed the reactivity of an M_r-70,000 (lamin A) and an M_r-60,000 (lamin C) protein (Fig. 4B); lamin C represents a mammalian splice variant of lamin A (6). However, the lamin-specific bands could not be clearly identified by immunoblot analysis in RacL11-, RacM24-, RacH-, and mock-infected cells after immunoprecipitation with the mixture of anti-lamin A antibodies, probably because the reactivity of the mouse IgG in Western blots covered the lamin-specific bands. In addition, in none of the cell lysates subjected to immunoprecipitation with the anti-IR6 antibody could a coprecipitation of type A lamins be observed (data not shown). The failure to detect lamin proteins in immunoblots after immunoprecipitation with the anti-IR6 antibody in RacL11-infected cells, although the RacL11 IR6 protein was specifically precipitated by the anti-lamin A antibodies in the same lysate, might be caused either by amounts of lamin A in the precipitates that were too low or by the relatively weak reactivity of these antibodies with mammalian lamins. The weak reactivity of the antibodies, which were produced against *Xenopus laevis* lamin proteins (7), to mammalian lamins in immunoblots was reflected by relatively low signal intensities of the M_r-70,000 and

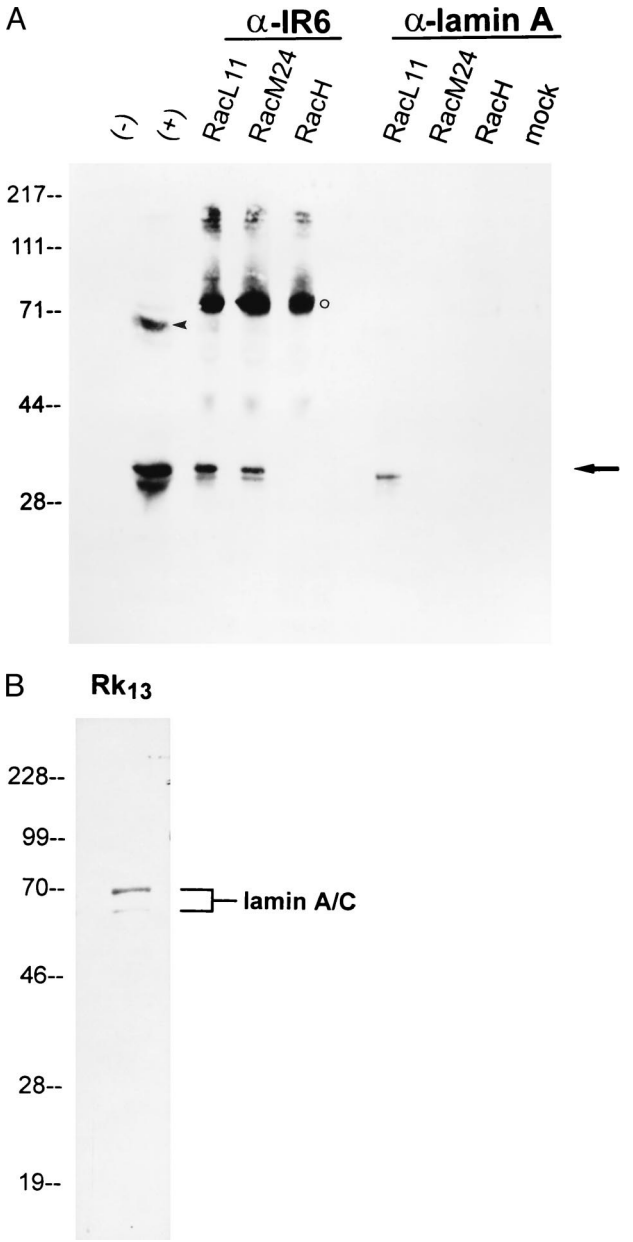

FIG. 4. (A) Western blot analysis of immunocomplexes obtained with anti-IR6 antibodies (α-IR6) or a mixture of anti-lamin A antibodies (α-lamin A). Lysates of cells that were infected with RacL11, RacM24, or RacH or were mock infected were prepared at 16 h p.i. and were subjected to immunoprecipitation with the indicated antibodies (α-IR6 or α-lamin A) as described in Materials and Methods. The immunocomplexes were separated by SDS–10% PAGE and transferred to nitrocellulose. Both IR6 and lamin immunoprecipitates were probed with the anti-IR6 antiserum. Lysates of RacL11-infected (+) and mock-infected cells (−) that were not subjected to immunoprecipitation were included as controls. The IR6-specific band is indicated by an arrow, and the putative IR6 dimer (19) in the positive control lysate (+) is marked with an arrowhead. The circle indicates rabbit IgG (M_r of 70,000 to 80,000). (B) Control Western blot of Rk_{13} cell lysates probed with anti-lamin A antibodies. Rk_{13} cell lysates were prepared and separated by SDS–10% PAGE, transferred to nitrocellulose, and probed with the mixture of anti-lamin A antibodies. Molecular weights of a prestained molecular weight marker (Gibco-BRL) are indicated in thousands.

especially the M_r-60,000 lamin protein (Fig. 4B). From the laser confocal microscopy and coimmunoprecipitation results with the anti-IR6 antibody and the anti-lamin A antibodies, as well as from similar coimmunoprecipitation experiments with anti-tubulin, anti-actin, anti-desmin, and anti-dynein antibodies which did not coprecipitate the IR6 protein (19, 20), it was concluded that the EHV-1 wild-type IR6 protein colocalizes with nuclear type A lamins at late times p.i. In contrast, the mutated IR6 protein expressed by RacM24, which no longer aggregates to the rod-like structures, did not colocalize with these components of the intermediate filament family at any time p.i.

The IR6 protein is involved in nucleocapsid egress. Previous observations have demonstrated that the inability of EHV-1 strains that either lack the IR6 gene (RacH) or express a mutated form of the protein (RacM24 and RacM36) to replicate efficiently at an elevated temperature of 40°C is caused by a defect in virus maturation and/or egress but not a failure to express individual late genes (20). To identify more precisely the role of the IR6 protein in EHV-1 replication, electron microscopical studies were performed. Edmin337 or Rk_{13} cells were infected at an MOI of 5 with either RacL11, RacM24, RacH, or the IR6-recombinant RacH virus HIR6-1 (20), and incubated at 37 or 40°C for 4 to 16 h. Infected cells were subsequently processed for electron microscopy. Examination of ultrathin sections of cells infected with the different viruses at 4 h p.i. revealed that infection of the cells occurred at both temperatures irrespective of the virus strain and the incubation temperature: few newly synthesized viral capsids could be observed in the nuclei of infected cells (data not shown). These data confirmed previous observations which indicated that an efficient expression of late gene products was observed in all virus strains at both 37 and 40°C (20). When infected cells were analyzed at 16 h p.i., no differences among the various viruses in nucleocapsid formation and translocation of newly synthesized virions to the cytoplasm or the extracellular space were observed at 37°C (Fig. 5A). Similarly, when cells infected with RacL11 were analyzed after incubation at 40°C for 16 h, an efficient production and translocation of capsids to the cytoplasm and to the extracellular and intercellular space were observed (Fig. 5C). In contrast, when ultrathin sections of cells infected with RacH at 40°C for 16 h were examined by electron microscopy, virtually no virions could be detected in the cytoplasm of infected cells or in the extra- and intercellular space. However, large amounts of immature and mature capsids (23, 24) were present in the nuclei of RacH-infected cells at the elevated temperature (Fig. 5B). As estimated from the inspection of a large number of different sections of RacH- and RacL11-infected cells, there was no marked difference in the total number of capsids produced at either 37 or 40°C. A similar pattern of virion distribution in infected cells was obvious after infection with RacM24 at the elevated temperature (data not shown). When cells infected at 40°C for 16 h with the engineered HIR6-1 virus (a RacH mutant expressing the wild-type IR6 protein [20]) were analyzed, efficient egress of capsids from the nuclei of the cells was observed, and the nucleocapsid egress of the IR6-recombinant RacH virus was indistinguishable from that of the RacL11 virus (Fig. 5D). These observations demonstrated that the temperature-sensitive (*ts*) phenotype of the RacH virus that lacks a functional IR6 gene is caused by a failure in capsid egress at the elevated temperature, and that the process of capsid egress is completely restored in the presence of one copy of the wild-type IR6 gene present in the HIR6-1 virus. In addition, only the wild-type form of the IR6 protein is able to confer the property of capsid egress at elevated temperatures to EHV-1 because the RacM24 virus expressing a mutated IR6 protein also exhibits a *ts* phenotype that is indistinguishable from that of RacH. Thus, a functional IR6 protein facilitates efficient EHV-1 capsid egress from nuclei of infected cells.

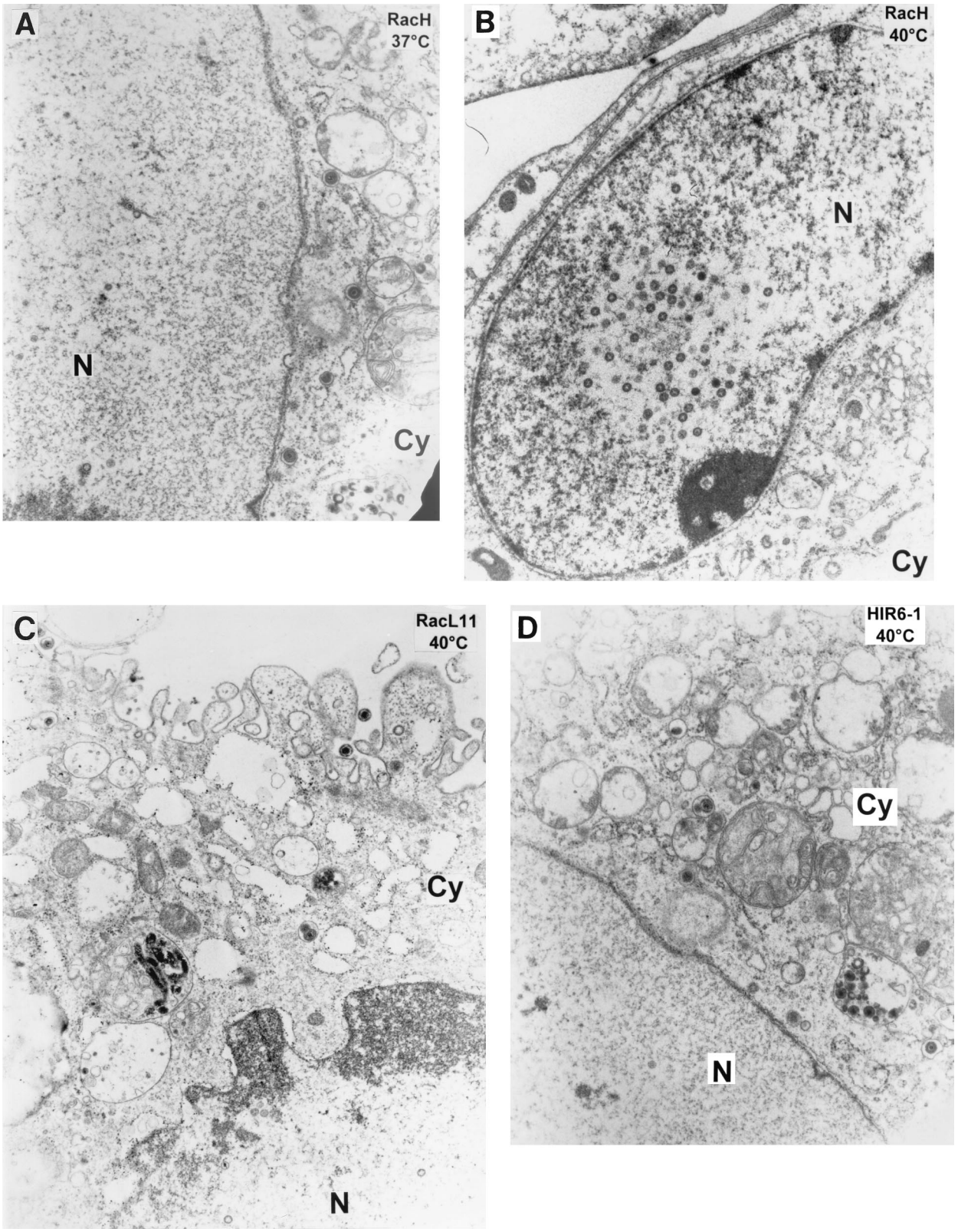

FIG. 5. Electron micrographs of Edmin337 cells infected with RacH virus at 37°C (A), and with RacH (B), RacL11 (C) or HIR6-1 (D) at 40°C. Cells were fixed at 16 h p.i. Ultrathin sections were prepared and viewed with a Zeiss electron microscope (EM 10C/CR). N, nucleus; Cy, cytoplasm. Whereas nucleocapsids in the nuclei and enveloped viruses in the cytoplasm and extracellular space are visible in RacH-infected cells at 37°C and in cells infected with RacL11 or HIR6-1 at 40°C, no virions in these compartments were observed in RacH-infected cells at 40°C. For size comparisons, capsids are approximately 120 nm in diameter.

TABLE 1. Total number of IR6-positive and β-galactosidase-positive cells after transfection[a]

Experiment no.[b]	pDIR6L/β-gal[c]	Ratio[d]	pDIR6M24/β-gal[c]	Ratio
1	837/26	32.2	125/45	2.8
2	929/33	28.2	56/37	1.5
3	321/12	26.8	211/57	3.7
4	745/36	20.7	54/51	1.1
5	709/41	17.3	40/24	1.7

[a] One microgram each of plasmid pDIR6L (wild-type IR6 gene of strain RacL11) or plasmid pDIR6M24 (mutated IR6 gene of strain RacM24) was cotransfected with pCβ$^+$ (1 μg) in 5×10^5 Rk_{13} cells by lipotransfection. The numbers of cells expressing β-galactosidase and the IR6 protein were determined by Bluo-Gal staining and immunofluorescence analysis, respectively. Values represent counts at 72 h after transfection.

[b] Five independent experiments were performed.

[c] Numbers represent total IR6-positive (before slash) and blue-staining cells (after slash). Counts were done with a fluorescence microscope (Zeiss) by randomly choosing 15 views (magnification, ×100).

[d] The ratio of cells expressing IR6 to cells expressing β-galactosidase.

The IR6 protein is transported from cell to cell and enters cells in the absence of virus infection. In the last series of experiments, the question of whether the EHV-1 IR6 protein is able to cross cellular boundaries independently of virus infection was addressed. Previous observations had suggested such a possibility because (i) after transfection of the wild-type IR6 gene into COS7 cells, almost every cell appeared to contain the IR6 protein at 96 h after transfection (19), and (ii) after infection of cells with RacL11 at an MOI of 0.1, the IR6 protein was detected in >60% of the cells at 10 h p.i. (22). To test the possibility of IR6 movement between cells and to determine whether the IR6 protein can enter cells from the outside, independently of virus infection, four different approaches were taken.

For the first, 5×10^5 Rk_{13} cells were cotransfected with 1 μg of pDIR6L or pDIR6M24 and 1 μg of pCβ$^+$. At different times after transfection (24, 48, and 72 h), cells were fixed with acetone, and the IR6 protein was detected with the monospecific anti-IR6 antiserum. To determine the number of β-galactosidase-positive cells compared with the IR6-positive cells, 15 randomly chosen views of transfected Rk_{13} cells (magnification, ×100) were scanned for IR6 and β-galactosidase staining at 72 h after transfection. After cotransfection of pDIR6L and pCβ$^+$, 12 to 41 cells expressed β-galactosidase, whereas 321 to 929 cells in the same views exhibited the typical rod-like expression pattern after immunofluorescent labeling that is indicative of the wild-type IR6 protein. These findings were confirmed in five independent experiments, and the ratio of IR6-positive cells to β-galactosidase-positive cells ranged from 17.3 to 32.2 (Table 1). In contrast, the number of IR6-positive cells after transfection of pDIR6M24 that encodes a mutated IR6 protein (72 h) also exceeded that of the β-galactosidase-positive cells, but by only 1.1- to 3.7-fold (Table 1). In addition to the determination of the total number of cells expressing β-galactosidase and the wild-type or mutated IR6 protein upon transient transfection, the distribution or "grouping" of positive cells was assessed. These results are summarized in Table 2. Whereas mainly single cells were shown to express β-galactosidase from 24 to 72 h after transfection, the RacL11 IR6 protein was mostly detected in adjacent cells, and some of the IR6-positive cells appeared to surround the original IR6-positive cell or the IR6-positive cells formed a "lineage" of cells as is shown in Fig. 6A for the 72-h time point. The grouping of IR6-positive cells became more obvious with time and, e.g., 33.9% of IR6-positive cells were clustered in groups of more than five cells at 72 h after transfection compared with 13.7% at the 24-h time point (Table 2). In contrast, β-galactosidase activity was detected in single or doublet cells throughout the observation period (Table 2). Similar to the behavior of the β-galactosidase-positive cells, the mutated RacM24 IR6 protein was detected in single cells or doublets only from 24 to

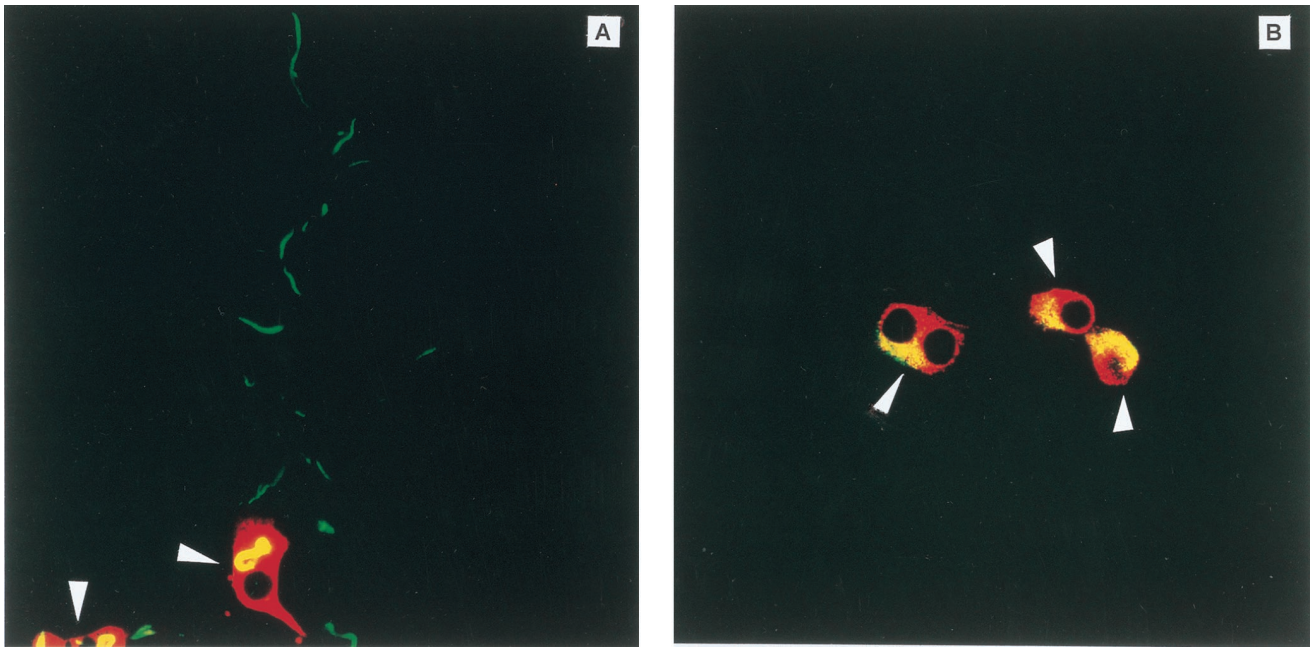

FIG. 6. Confocal laser scanning image of Rk_{13} cells cotransfected with either wild-type (RacL11) (A) or mutated (RacM24) IR6 gene (B) and reporter plasmid pCβ$^+$. The IR6 protein and β-galactosidase were detected at 72 h after transfection by double immunofluorescent staining as described in Materials and Methods. The cells were analyzed by confocal laser microscopy. IR6 staining (green) and β-galactosidase staining (red) are shown. β-Galactosidase-expressing cells are marked with an arrowhead.

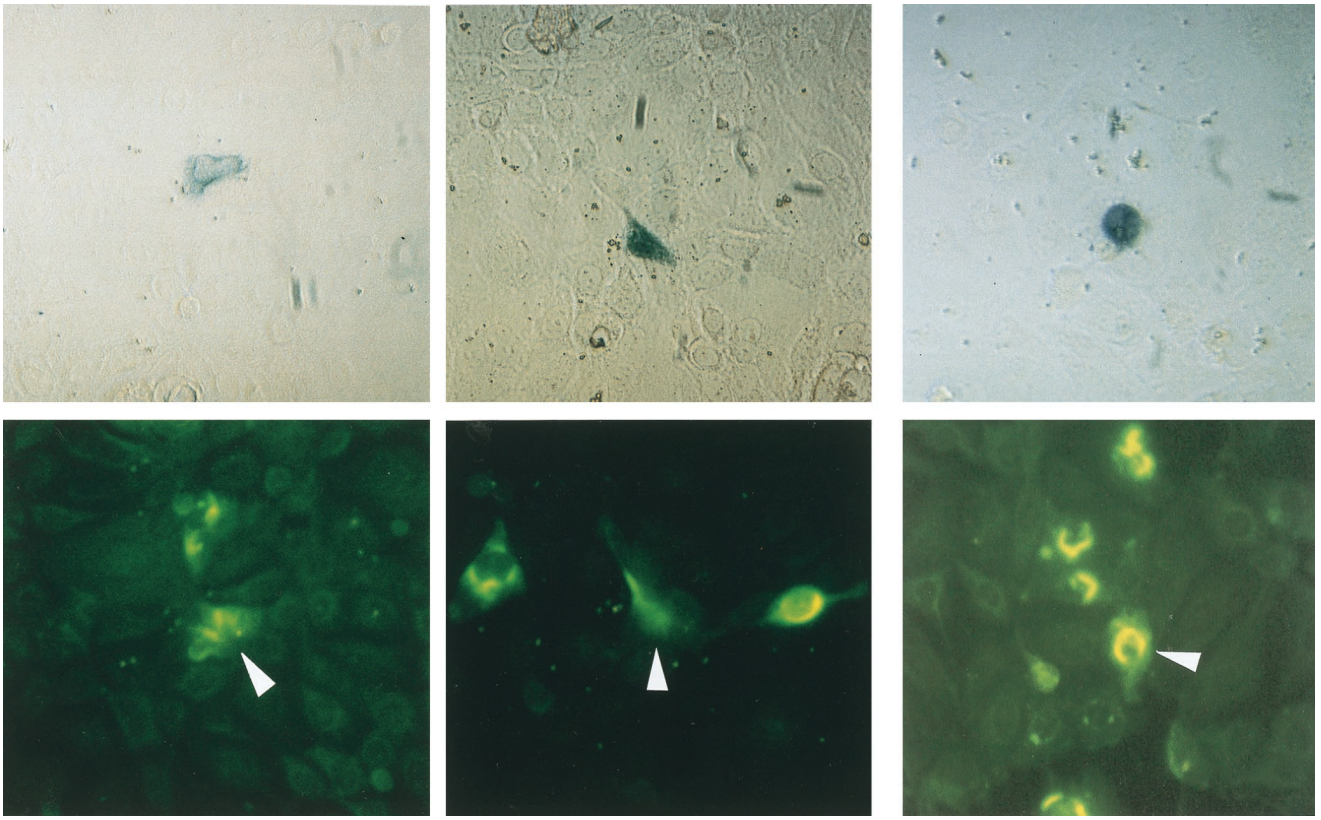

FIG. 7. Photographs of Rk_{13} cells infected with the gB-negative RacL11 virus mutant (L11ΔgB) that expresses β-galactosidase. Infected cells were fixed at 10, 20, or 36 h p.i. Top panels show Bluo-Gal staining of L11ΔgB-infected cells, and bottom panels show immunofluorescence labeling of the IR6 protein in the same views. Photographs were taken with a Zeiss Axiovert 25 microscope. Magnification, ×240. Infected cells are marked with an arrowhead.

72 h after transfection and mostly colocalized with cells expressing β-galactosidase. The detection of the mutated IR6 protein in transfected cells is shown for the 72-h time point in Figure 6B.

For the second approach, the results of IR6 transport from cell to cell in the absence of virus infection that were obtained by the transient transfection experiments were confirmed by analyzing a gB-negative virus mutant of RacL11 that expresses β-galactosidase. This mutant virus is unable to spread from cell to cell (15). Noncomplementing Rk_{13} cells were infected with gB-negative L11ΔgB (200 PFU per 60-mm dish), and at 10 to 36 h p.i., cells were fixed with acetone and stained by indirect IF using the anti-IR6 antiserum and an anti-rabbit IgG FITC conjugate. Infected cells were visualized with Bluo-Gal staining. Consistent with earlier findings (15), only single infected cells were observed at each time point after infection with L11ΔgB as demonstrated by the presence of single blue-staining cells (Fig. 7). In contrast, IR6-positive cells were observed to surround the infected cell or to form the lineages starting from a single infected cell. In some cases, the IR6-positive cells appeared to be not directly adjacent to each other, but the overall picture of IR6 distribution was comparable to that described after transient transfection and immunofluorescence labeling of the IR6 protein (Fig. 7). These results were confirmed in similar experiments, where infection of cells with L11ΔgB was detected with an anti-β-galactosidase MAb followed by an anti-mouse IgG TRITC conjugate. IR6-specific labeling was detected by confocal laser scan microscopy in uninfected cells that were adjacent to cells infected with the L11ΔgB virus. As described above, the detection of the IR6 protein in uninfected cells was readily apparent from 10 h p.i. (data not shown).

In the third series of experiments, migration of the wild-type IR6 protein was investigated in mixed cell cultures containing pDIR6L-transfected TCgBf cells that constitutively express EHV-1 gB (15) and normal Rk_{13} cells. It could be clearly

TABLE 2. Allocation of reactive cells at different times after cotransfection[a]

Group[b]	% IR6-positive cells			% β-Gal-positive cells		
	24 h	48 h	72 h	24 h	48 h	72 h
1	44.8[c]	17.9	18.8	92.6	94.4	91.8
2	41.5	54.3	47.3	7.4	5.6	8.2
3	13.7	27.8	33.9	0	0	0
Total	100.0	100.0	100.0	100.0	100.0	100.0

[a] Counts were performed in a total of 75 views (magnification, ×100). The numbers of IR6-positive and β-galactosidase-positive cells were counted in 15 randomly chosen views for each of five independent experiments. One microgram each of plasmid pDIR6L and $pC\beta^+$ was lipotransfected into 5×10^5 Rk_{13} cells.

[b] Three different groups of positive cells were differentiated as follows: group 1, two or less adjacent positive cells ($n \leq 2$); group 2, three or four adjacent positive cells ($2 < n \leq 4$); group 3, five or more adjacent positive cells ($n \geq 5$).

[c] Total numbers of positive cells were determined and used to assign cells to the respective groups described above. Numbers of cells in each of the groups were divided by the total number of positive cells, and percentages were calculated by multiplying by 100.

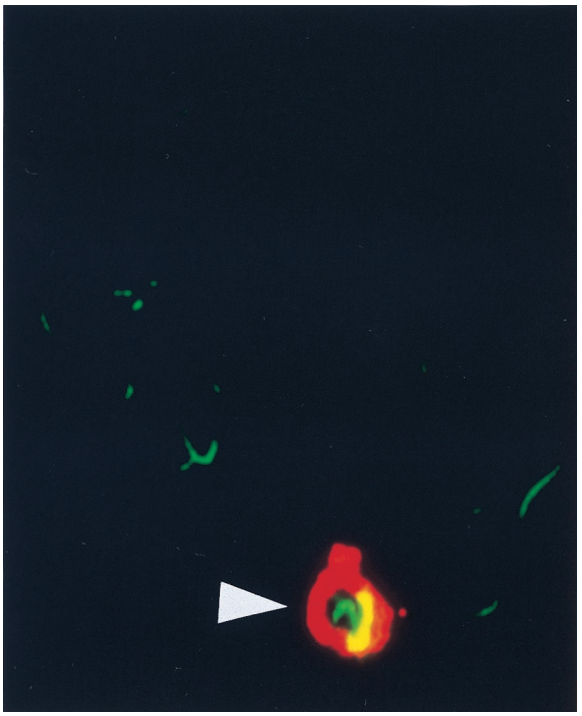

FIG. 8. Confocal laser scanning image of TCgBf cells that had been transfected with pDIR6L and were mixed with Rk_{13} cells. Cells were mixed at a ratio of approximately 1:30 (1 transfected TCgBf cell per 30 normal Rk_{13} cells). The IR6 protein was detected with the rabbit antibody and visualized with anti-rabbit IgG FITC, while EHV-1 gB was detected with MAb 4B6 (15) and visualized with anti-mouse IgG TRITC. Overlay of IR6 and gB fluorescences are shown. A TCgBf cell containing IR6 protein is marked with an arrowhead.

demonstrated that IR6-specific rod-like structures were observed in a small number of Rk_{13} cells, which did not react with the gB-specific MAb 4B6 that was used to identify TCgBf cells. These IR6-positive Rk_{13} cells were adjacent to transfected TCgBf cells demonstrating transport between different cell types (Fig. 8). These results were confirmed by the reciprocal experiment in which Rk_{13} cells transfected with pDIR6L were mixed with TCgBf cells (data not shown).

Lastly, the ability of the wild-type and mutant IR6 proteins to enter cells from the extracellular space was addressed. Rk_{13} cells that had been transfected with either pDIR6L or pDIR6M24 were harvested at 72 h after transfection and lysed with 0.4 M NaCl (4). The cell lysates were dialyzed against DMEM and added to Rk_{13} cells seeded in 96-well plates (cell lysates corresponding to 3×10^3 cells were added per well). At different times (1 to 48 h) after addition of the transfected-cell lysates, indirect IF with the anti-IR6 antibody was performed. The results are summarized in Table 3. In Rk_{13} cells that had been overlaid with wild-type IR6-transfected cell lysates, IR6-specific staining was observed in approximately 2 to 4% of the cells from 1 h p.i., whereas no IR6-specific fluorescence could be demonstrated in Rk_{13} cells incubated with mutated IR6 protein encoded by pDIR6M24. The percentage of IR6-positive cells did not increase with time after the addition of the pDIR6L lysate (Table 3). These observations indicated that the wild-type IR6 protein is able to enter cells from the medium.

DISCUSSION

This study describes experiments that were performed to characterize the properties of the EHV-1 IR6 protein. Though nonessential for virus growth (19) and absent in the prototype of the alphaherpesviruses, HSV-1, the IR6 protein is involved in EHV-1 virulence (20), and homologs of the protein have been identified in EHV-4 as well as BHV-1 and CHV (11, 14, 26, 31), suggesting that IR6 homologous proteins might be important for perpetuation of virus infection in vivo. The formation of rod-like structures induced by the wild-type IR6 protein that is reminiscent of structures formed by proteins that make up the cellular architecture led us and other investigators to address the possible interaction of the IR6 protein with members of the filament families. While the cellular protein(s) associated with the IR6 protein was not identified in these previous studies (17, 19, 29), the laser confocal microscopy data and the coimmunoprecipitation experiments presented in this study demonstrate a colocalization of the wild-type IR6 protein and cellular type A lamins. However, we were not able to demonstrate precipitation of lamin proteins from cell lysates by using a glutathione *S*-transferase–IR6 fusion protein although the fusion protein itself was precipitated as demonstrated by both Coomassie blue staining and Western blot analysis (19, 22). In addition, we view it as unlikely that unspecific precipitation of the IR6 protein by the anti-lamin antibodies occurs because no precipitation of other EHV-1 structural proteins, such as gD or gB, by the anti-lamin antibodies could be demonstrated by immunoblotting (data not shown). Similarly, the wild-type IR6 protein was not coprecipitated by using antibodies directed against other filament proteins such as tubulin, actin, or desmin (19). Nevertheless, the interaction of the IR6 protein with lamins is a very late event in virus infection and remains restricted to approximately 10% of infected cells. Also, the rod-like structures do not contain lamin proteins in all cases. It is therefore possible that the IR6-lamin interaction is restricted to specific cell types or to cells that are in a certain stage of the cell cycle. At present, it is difficult to interpret the relationships between the formation of the IR6 rod-like structures, phosphorylation of the IR6 protein, and the interaction of the IR6 protein with type A lamins with an efficient export of nucleocapsids that is less efficient (i) in the absence of the IR6 protein (EHV-1 strain RacH), and (ii) in the presence of a mutated form of the abundantly produced protein encoded by RacM24 and RacM36 (reference 20 and this study). The ability of viruses that are devoid of a wild-type IR6 protein to replicate efficiently at an incubation temperature of 37°C but not at 40°C suggests that the IR6 function can be compensated by another viral or cellular protein(s) in cultured cells. The fact that RacM24, RacM36, and RacH are

TABLE 3. Cells containing IR6 protein after addition of NaCl extract[a]

Hours after addition of extract	% of cells that were IR6 positive after transfection with:	
	pDIR6L extract	pDIR6M24 extract
1	3.5 ± 1.9[b]	0[c]
6	2.2 ± 1.1	0
12	4.1 ± 2.6	0
24	3.1 ± 0.8	0
48	2.8 ± 1.3	0

[a] NaCl extracts of Rk_{13} cells transfected with either pDIR6L or pDIR6M24 were prepared as described in the text. Rk_{13} cells seeded in a 96-well plate were overlaid with one of the extracts. An extract corresponding to approximately 3×10^3 cells per well containing 1×10^4 freshly seeded Rk_{13} cells was added.

[b] Percentages of IR6-positive cells were determined after labeling with anti-IR6 antiserum. Nuclei were stained with propidium iodide. Values are means ± standard deviations of four wells per time point.

[c] A value of 0 indicates that less than 10 cells per well showed fluorescence.

apathogenic for the natural host and laboratory animals (8, 12, 20) may also support the interpretation that the IR6 protein exerts a cell type-specific function. Ongoing studies to elucidate the in vivo function of the IR6 protein include the generation of IR6-transgenic animals.

A striking feature of the wild-type IR6 protein is its ability to cross cellular boundaries in the absence of virus infection. The results from a series of independent experiments clearly demonstrated that the wild-type IR6 protein is able to move from cell to cell in the absence of infection because (i) the number of IR6-positive cells exceeded that of the cells expressing a reporter gene by 17- to more than 30-fold after transient transfection, (ii) the wild-type IR6-positive cells appeared to form groups or lineages of cells, (iii) IR6-positive cells surrounded cells infected with a gB-negative RacL11 virus mutant that is defective in cell-to-cell spread, (iv) migration of wild-type IR6 protein between different cells was demonstrated, and (v) wild-type IR6 protein entered cells from the extracellular space. In contrast, the mutated IR6 protein encoded by pDIR6M24 was severely impaired in these properties inasmuch as the numbers of IR6-positive cells only marginally exceeded that of the β-galactosidase-positive cells at any time point after transient transfection, and no migration between cell types or uptake of mutated IR6 from the medium could be demonstrated.

The intrinsic property of a herpesviral protein to spread from cell to cell independently of virus infection is not unprecedented as the HSV-1 tegument protein VP22 also exhibits this property. It must be noted, however, that the intercellular transport of the IR6 protein does not appear to be as efficient as that of VP22. In addition, it has been shown that purified VP22 protein can enter cells via an actin-dependent transport mechanism, making it a good candidate for protein delivery to target cells (4). Although the IR6 protein exhibits similar features, the exact mechanism by which the IR6 protein is transported from cell to cell, is taken up from the medium, and moves inside cells is not known. Unlike the HSV-1 VP22 tegument protein, however, this transport appears not to be dependent on the actin cytoskeleton, because IR6 rod formation and transport were not affected by cytochalasin D treatment in Rk_{13} or COS7 cells (19, 22). The existence of herpesviral proteins that are transported to neighboring cells might point to a similar mechanism by which yet-uninfected cells are prepared for subsequent infection via a virus-encoded messenger to facilitate infection, perhaps by interference with proteins involved in the cell's architecture and division machinery. An alternative explanation for IR6 movement to neighboring cells may be, however, that certain cell types or cells in a specific phase of the cell cycle are rendered resistant to infection after uptake of the IR6 protein to allow virus replication in fully permissive cells only. These hypotheses are currently being tested and are consistent with the fact that both the HSV-1 VP22 and EHV-1 IR6 proteins are (very) early gene products which are produced starting at 2 to 4 h p.i. (4, 17, 19).

In sum, this report describes the characterization of the EHV-1 IR6 protein on a cellular and molecular level. These data and our previously published observations indicate that the aggregation of the IR6 to filamentous structures (i) is an important factor that determines EHV-1 virulence, (ii) is responsible for its colocalization with nuclear type A lamins, (iii) facilitates efficient egress of viral capsids from nuclei of infected cells, and (iv) enables the viral protein to be transported from cell to cell independent of virus infection.

ACKNOWLEDGMENTS

We are indebted to Georg Krohne, Theodor-Boveri-Institute, University of Würzburg, Germany, for providing anti-lamin monoclonal antibodies.

This study was supported by a grant from the Mehl-Mülhens-Stiftung to N.O. and O.-R.K. and by NIH grant AI 22001 to D.J.O.

REFERENCES

1. **Allen, G. P., and J. T. Bryans.** 1986. Molecular epizootiology, pathogenesis, and prophylaxis of equine herpesvirus-1 infections. Prog. Vet. Microbiol. Immunol. **2:**78–144.
2. **Breeden, C. A., R. R. Yalamanchili, C. F. Colle, and D. J. O'Callaghan.** 1992. Identification and transcriptional mapping of genes encoded at the IR/Us junction of equine herpesvirus type 1. Virology **191:**649–660.
3. **Colle, C. F., and D. J. O'Callaghan.** 1996. Localization of the Us protein kinase of equine herpesvirus type 1 is affected by the cytoplasmic structures formed by the novel IR6 protein. Virology **220:**424–435.
4. **Elliott, G., and P. O'Hare.** 1997. Intercellular trafficking and protein delivery by a herpesvirus structural protein. Cell **88:**223–233.
5. **Flowers, C. C., and D. J. O'Callaghan.** 1992. Equine herpesvirus 1 glycoprotein D: mapping of the transcript and a neutralization epitope. J. Virol. **66:**6451–6460.
6. **Fuchs, E., and K. Weber.** 1994. Intermediate filaments: structure, dynamics, function and disease. Annu. Rev. Biochem. **63:**345–382.
7. **Höger, T., G. Krohne, and J. A. Kleinschmidt.** 1991. Interaction of Xenopus lamins LA and LII with chromatin in vitro mediated by a sequence element in the carboxyterminal domain. Exp. Cell Res. **197:**280–289.
8. **Hübert, P. H., S. Birkenmaier, H. J. Rziha, and N. Osterrieder.** 1996. Alterations in the equine herpesvirus type-1 (EHV-1) strain RacH during attenuation. J. Vet. Med. B **43:**1–14.
9. **Kyhse-Andersen, J.** 1984. Electroblotting of multiple gels: a simple apparatus without tank for rapid transfer of proteins from polyacrylamide gels to nitrocellulose. J. Biochem. Biophys. Methods **10:**203–210.
10. **Laemmli, U. K.** 1970. Cleavage of structural proteins during the assembly of the head of bacteriophage T4. Nature **227:**680–685.
11. **Leung Tack, P., J. C. Audonnet, and M. Riviere.** 1994. The complete DNA sequence and the genetic organization of the short unique region (US) of the bovine herpesvirus type 1 (ST strain). Virology **199:**409–421.
12. **Mayr, A., J. Pette, K. Petzoldt, and K. Wagener.** 1968. Untersuchungen zur Entwicklung eines Lebendimpfstoffes gegen die Rhinopneumonitis (Stutenabort) der Pferde. J. Vet. Med. B **15:**406–418.
13. **Mumford, J. A., D. A. Hannant, D. M. Jessett, T. O'Neill, K. C. Smith, and E. N. Ostlund.** 1995. Abortigenic and neurological disease caused by experimental infection with equid herpesvirus-1, p. 261–275. *In* H. Nakajima and W. Plowright (ed.), Proceedings, 7th International Conference of Equine Infectious Diseases. R&W Publications, Newmarket, United Kingdom.
14. **Nagesha, H. S., B. S. Crabb, and M. J. Studdert.** 1993. Analysis of the nucleotide sequence of five genes at the left end of the unique short region of the equine herpesvirus 4 genome. Arch. Virol. **128:**143–154.
15. **Neubauer, A., B. Braun, C. Brandmüller, O.-R. Kaaden, and N. Osterrieder.** 1997. Analysis of the contributions of the equine herpesvirus 1 glycoprotein gB homolog to virus entry and direct cell-to-cell spread. Virology **227:**281–294.
16. **Nigg, E. A.** 1992. Assembly-disassembly of the nuclear lamina. Curr. Opin. Cell Biol. **4:**105–109.
17. **O'Callaghan, D. J., C. F. Colle, C. C. Flowers, R. H. Smith, J. N. Benoit, and C. A. Bigger.** 1994. Identification and initial characterization of the IR6 protein of equine herpesvirus 1. J. Virol. **68:**5351–5364.
18. **O'Callaghan, D. J., G. A. Gentry, and C. C. Randall.** 1983. The equine herpesviruses, p. 215–318. *In* B. Roizman (ed.), The herpesviruses. Plenum Publishing Corporation, New York, N.Y.
19. **Osterrieder, N., V. R. Holden, C. Brandmüller, A. Neubauer, O.-R. Kaaden, and D. J. O'Callaghan.** 1996. The equine herpesvirus 1 IR6 protein is nonessential for virus growth in vitro and modified by serial virus passage in cell culture. Virology **217:**442–451.
20. **Osterrieder, N., A. Neubauer, C. Brandmüller, O.-R. Kaaden, and D. J. O'Callaghan.** 1996. The equine herpesvirus 1 IR6 protein influences virus growth at elevated temperature and is a major determinant of virulence. Virology **226:**243–251.
21. **Osterrieder, N., R. Wagner, C. Brandmüller, P. Schmidt, H. Wolf, and O.-R. Kaaden.** 1995. Protection against EHV-1 challenge infection in the murine model after vaccination with various formulations of recombinant glycoprotein gp14 (gB). Virology **208:**500–510.
22. **Osterrieder, N., and A. Neubauer.** 1998. Unpublished observations.
23. **Perdue, M. L., J. C. Cohen, M. C. Kemp, C. C. Randall, and D. J. O'Callaghan.** 1975. Characterization of three species of nucleocapsids of equine herpes virus type 1 (EHV-1). Virology **64:**187–204.
24. **Perdue, M. L., J. C. Cohen, C. C. Randall, and D. J. O'Callaghan.** 1976. Biochemical studies of the maturation of herpesvirus nucleocapsid species. Virology **74:**194–208.

25. **Peter, M., J. Nakagawa, M. Doree, J. C. Labbe, and E. A. Nigg.** 1990. In vitro disassembly of the nuclear lamina and M phase-specific phosphorylation of lamins by cdc2 kinase. Cell **61:**591–602.
26. **Remond, M., P. Sheldrick, F. Lebreton, P. Nardeux, and T. Foulon.** 1996. Gene organization in the UL region and inverted repeats of the canine herpesvirus genome. J. Gen. Virol. **77:**37–48.
27. **Sambrook, J., E. F. Fritsch, and T. Maniatis.** 1989. Molecular cloning: a laboratory manual. Cold Spring Harbor Laboratory Press, Cold Spring Harbor, N.Y.
28. **Schmidt, M., M. Tschödrich-Rotter, R. Peters, and G. Krohne.** 1994. Properties of fluorescently labeled Xenopus lamin A in vivo. Eur. J. Cell Biol. **65:** 70–81.
29. **Sun, Y., A. R. MacLean, and S. M. Brown.** 1995. Identification and characterization of the protein product of gene 67 in equine herpesvirus type 1 strain Ab4. J. Gen. Virol. **76:**541–550.
30. **Telford, E. A. R., M. S. Watson, K. McBride, and A. J. Davison.** 1992. The DNA sequence of equine herpesvirus-1. Virology **189:**304–316.
31. **Telford, E. A. R., M. S. Watson, J. Perry, A. A. Cullinane, and A. J. Davison.** 1998. The DNA sequence of equine herpesvirus-4. J. Gen. Virol. **79:**1197–1203.